



Article

# 3D Printed Fully Recycled TiO<sub>2</sub>-Polystyrene Nanocomposite Photocatalysts for Use against Drug Residues

Maria Sevastaki <sup>1,2</sup>, Mirela Petruta Sucheai <sup>3,4,\*</sup>  and George Kenanakis <sup>1,\*</sup> 

<sup>1</sup> Institute of Electronic Structure and Laser, Foundation for Research & Technology-Hellas, N. Plastira 100, 70013 Heraklion, Crete, Greece; msevastaki@iesl.forth.gr

<sup>2</sup> Department of Chemistry, University of Crete, 71003 Heraklion, Crete, Greece

<sup>3</sup> National Institute for Research and Development in Microtechnologies (IMT-Bucharest), 1 26 A, Erou Iancu Nicolae Street, P.O. Box 38-160, 023573 Bucharest, Romania

<sup>4</sup> Center of Materials Technology and Photonics, Hellenic Mediterranean University, 71004 Heraklion, Crete, Greece

\* Correspondence: mira.sucheai@imt.ro (M.P.S.); gkenanak@iesl.forth.gr (G.K.)

Received: 12 October 2020; Accepted: 26 October 2020; Published: 28 October 2020



**Abstract:** In the present work, the use of nanocomposite polymeric filaments based on 100% recycled solid polystyrene everyday products, enriched with TiO<sub>2</sub> nanoparticles with mass concentrations up to 40% *w/w*, and the production of 3D photocatalytic structures using a typical fused deposition modeling (FDM)-type 3D printer are reported. We provide evidence that the fabricated 3D structures offer promising photocatalytic properties, indicating that the proposed technique is indeed a novel low-cost alternative route for fabricating large-scale photocatalysts, suitable for practical real-life applications.

**Keywords:** metal oxide nano-structures; titanium dioxide (TiO<sub>2</sub>); photocatalysis; paracetamol; 3D printing; fused filament fabrication (FFF); fused deposition modeling (FDM)

## 1. Introduction

For many years, human activities have polluted the environment in many ways; several organic residuals originating from highly toxic pollutants such as pharmaceuticals can be found in water, comprising a critical health and environmental issue [1–3]. In many cases, unused, expired and residual pharmaceuticals are discharged into the sewerage system, burdening the aquifer. Moreover, these compounds can also be discharged into the environment through the metabolism of human bodies [4–8]. As a result, pharmaceuticals have been found in sewage, surface and ground water in many countries [6,8,9].

The most common methods used to overcome this problem include the return of medicines to pharmacies and not throwing expired medicinal products in the sewer, as well as biological degradation, chlorination or ozonation, but these are not efficient enough to remove these compounds from the treated water [10–12]. These drugs residues must be eliminated using an oxidation method, and advanced heterogeneous photocatalysis seems to be one of the most promising approaches, since it implies the use of an inert catalyst, non-hazardous oxidants and ultraviolet (UV) and/or visible light input [13–25].

Heterogeneous photocatalysis using TiO<sub>2</sub> is a method generating free radical •OH using atmospheric air instead of O<sub>3</sub> or H<sub>2</sub>O<sub>2</sub>, significantly reducing processing costs. The process takes place at ambient conditions and leads to the complete decomposition of both liquid and gaseous pollutants [26,27]. The greatest advantage of this method is that an environmentally friendly catalyst which is widely available, inexpensive, non-toxic, and photo-stable with respect to other photocatalysts

is readily available and readily regenerable for the purpose of reuse, maintaining equally high performance for a large number of catalytic cycles [13–17,26]. Several studies have shown that titanium dioxide (TiO<sub>2</sub>) is the most potent semiconductor for the oxidative destruction of organic compounds. TiO<sub>2</sub> has, in addition to its large photocatalytic activity, greater resistance to corrosion and photo-corrosion, resulting in the possibility of recycling [28].

The disadvantage of photocatalysis when the semiconductor is used in the form of a powder is the need to remove it after the end of the treatment [29,30]. For this reason, international efforts are focused on photocatalytic systems, where the catalyst is used in the form of a film on inert substrates to eliminate the stage of powder removal [31–35]. Over and above that, photocatalytic efficiency increases with effective surface area, and consequently a nanostructured photocatalyst is beneficial. However, solid catalysts' samples, such as thin films or nanostructured ones, in most cases cannot exceed an overall size of a few centimeters, due to the limitation of the fabrication techniques, limiting their potential use in real-life applications.

In the last few years, 3D printing technology become of great interest in several fields of research, such as medicine, chemistry and materials science, as an effective, fancy, quick and low-cost route for the production of 3D large-size samples [36–40]. The most common technique is fused deposition modeling (FDM) in which polymers are the usual materials used as filaments. It should be noted that although there are several reports on 3D structures for novel environmental applications [41–43], there are only a few in which custom-made filaments (with nanoparticles of inorganic materials into a polymeric matrix) are used in combination with FDM technology, i.e., in [44,45], and none for drug-residuals' removal by photocatalysis.

This work discusses an investigation of the photocatalytic degradation of paracetamol (also known as acetaminophen, APAP), a medicine available in a huge number of countries worldwide, used to treat pain and fever, using 3D-printed photocatalysts enriched with 20% *w/w* nanostructured TiO<sub>2</sub>. It is worth mentioning that the polymeric filaments used to produce these 3D-printed photocatalysts are based on 100% recycled solid polystyrene (PS) everyday products, such as containers, lids, CD cases etc., following an eco-friendly environmental approach. APAP was chosen for this study due to its high occurrence as a pharmaceutical pollutant in environment. As shown in many studies, it was found worldwide in almost all kinds of water source as well in the soil [46]. APAP is reported to be one of the most frequently detected pharmaceuticals in sewage treatment plant effluents [47]. The increasing concentrations of APAP together with other emerging contaminants result in the occurrence of toxic phenomena in non-target species present in receiving aquatic environments. An excellent review regarding the toxic effects of environmental APAP is presented in Ref. [48].

The present experimental results provided strong evidence that the proposed fully recycled 3D printed photocatalysts are good candidates against the degradation of APAP drug residues, reaching an efficiency of almost 75% of a 100 ppm APAP aqueous solution under UV irradiation for 20 min, and ~60% after three cycles of reuse in 200 ppm APAP aqueous solutions, respectively.

## 2. Experimental Details

### 2.1. Synthesis of the Metal Oxide Polymeric Nanocomposites

First, several everyday PS products, such as containers, lids, CD cases etc. were ground using an IKA A11 Basic Analytical Mill (IKA-Werke GmbH and Co. KG, Staufen, Germany) equipped with a high-grade stainless-steel beater, coated with chromium carbide. Recycled grinded PS powder/beads of ~0.2 mm diameter were dissolved in toluene (Merck KGaA, Darmstadt, Germany) (in a sealed bottle, under continuous stirring for 2 h) to create a 20% *w/w* solution. The resultant solution was stirred for 24 h at room temperature using a magnetic stirrer to yield a homogeneous, milky solution.

Subsequently, 2 g and 4 g of commercially available TiO<sub>2</sub> nanoparticles (TiO<sub>2</sub> P25 with a mean particle size of ~25 nm, obtained from Evonic Industries AG, Essen, Germany) were introduced in

10 mL of the PS/toluene solution mentioned above under stirring at 40 °C for 30 min, in order to obtain the TiO<sub>2</sub> homogeneous suspensions with 20% *w/w* and 40% *w/w* concentration in PS, respectively.

Each of the TiO<sub>2</sub> homogeneous suspensions was transferred to 200 mL of ethanol (95% purity; Merck KGaA, Darmstadt, Germany), to form a dense precipitate, which consisted of the PS and the suspended metal oxide nanoparticles. After formation, the precipitate was collected and dried at 60 °C for 24 h using a typical laboratory oven (Memmert UNP 500 Memmert GmbH + Co., Schwabach, Germany). Using the procedure above, 20 g of 20% *w/w* TiO<sub>2</sub>/PS, and 20 g 40% *w/w* TiO<sub>2</sub>/PS solid nanocomposite solutions were produced, respectively.

## 2.2. Filament Production

The produced TiO<sub>2</sub>/PS solid nanocomposite solutions were cut in ~2–3 mm<sup>2</sup> pieces, and forwarded to a “Noztek Pro” (Noztek, Shoreham, West Sussex, UK) high temperature extruder, and processed at 240 °C, in order to transform them to a cylindrical filament with a diameter of 1.75 ± 0.15 mm, suitable for 3D-printing. All extrusion parameters, such as extrusion velocity and temperature, were optimized towards the production of a uniform continuous cylindrical cord, with an overall length of ~5 m.

## 2.3. Production of 3D-Printed Photocatalytic Structures

Flat, rectangular-shaped (10 mm × 10 mm × 1 mm) 3D structures were designed using “Tinkercad”, a free online 3D design and 3D printing software from Autodesk Inc (Mill Valley, CA, USA). A dual-extrusion FDM-type 3D printer (Makerbot Replicator 2X; MakerBot Industries, Brooklyn, NY, USA) was used for the direct fabrication of TiO<sub>2</sub>/PS nanocomposite photocatalytic samples, using the PS/TiO<sub>2</sub> nanocomposite filaments described above. The FDM process of building a solid object involves heating of the fed filament and pushing it out layer-by-layer through a heated (240 °C) nozzle (0.4 mm inner diameter) onto a heated surface (80 °C), via a computer controlled three-axis positioning system (with a spatial resolution of approximately 100 μm in the z-axis and 11 μm in x and y).

## 2.4. Characterization and Photocatalytic Experiments

X-ray diffraction (XRD) measurements were performed in order to determine the crystalline structure of the 3D-printed samples, using a Rigaku RINT 2000 (Rigaku, Tokyo, Japan) diffractometer with Cu Kα (λ = 1.5406 Å) X-rays for 2θ = 20.00–60.00° for TiO<sub>2</sub>/PS nanocomposite-based samples and a step time 60°/sec.

Furthermore, Raman spectroscopy measurements were performed at room temperature using a Horiba LabRAM HR Evolution (HORIBA FRANCE SAS, Longjumeau, France) confocal micro-spectrometer, in backscattering geometry (180°), equipped with an air-cooled solid-state laser operating at 532 nm with 100 mW output power. The laser beam was focused on the samples using a 10× Olympus (OLYMPUS corporation, Tokyo, Japan) microscope objective (numerical aperture of 0.25), providing ~14 mW power on each sample. Raman spectra over the 100–700 cm<sup>-1</sup> wavenumber range (with an exposure time of 5 s and 3 accumulations) were collected by a Peltier cooled CCD (1024 × 256 pixels) detector (HORIBA FRANCE SAS, Longjumeau, France) at -60 °C, with a resolution better than 1 cm<sup>-1</sup>, achieved thanks to an 1800 grooves/mm grating and an 800 mm focal length. Test measurements carried out using different optical configuration, exposure time, beam power and accumulations in order to obtain sufficiently informative spectra using a confocal hole of 100 μm, but ensuring to avoid alteration of the sample, while the high spatial resolution allowed us to carefully verify the sample homogeneity. The wavelength scale was calibrated using a Silicon standard (520.7 cm<sup>-1</sup>) (Silchem Handelsgesellschaft mbH, Freiberg, Germany) and the acquired spectra were compared with scientific published data and reference databases, such as Horiba LabSpec 6 (HORIBA FRANCE SAS, Longjumeau, France).

The photocatalytic activity of the 3D-printed samples was studied by means of the reduction of APAP in aqueous solution, which is a well-known pharmaceutical product that has been used as a model organic to probe the photocatalytic performance of photocatalysts [4,5,7,8]. The investigated samples were placed in a vertical custom-made quartz cell, and the whole setup (cell + solution + sample) was illuminated up to 60 min using an HPK 125 W Philips UV lamp centered at 365 nm (msscientific Chromatographie-Handel GmbH, Berlin, Germany) with a light intensity of  $\sim 6.0$  mW/cm<sup>2</sup>. The concentration of APAP (degradation) was monitored by UV-Vis spectroscopy in absorption mode (absorption at  $\lambda_{\text{max}}$ , 665 nm), using a K-MAC SV2100 (K-MAC, Daejeon, Korea) spectrophotometer over the wavelength range of 220–800 nm. In such way, UV-Vis absorption data were collected at 0, 10, 20, 30 and 40 min, while the quantification of the APAP removal (and hence the remaining APAP concentration) was estimated by calculation of the area below the main APAP peak in the range of 220–320 nm. Additional blank experiments (photolysis) without a catalyst were also performed as well as APAP adsorption experiments in the dark.

### 3. Results and Discussion

In order to verify the nominal TiO<sub>2</sub> loading in PS filaments and 3D-printed nanocomposites, a type of thermogravimetric method was used. A small piece of each sample on a quartz substrate, was weighted and was heated at  $\sim 900$  °C in order to burn all organics and polymeric residuals, then weighed again. Since TiO<sub>2</sub> is not affected at all at such temperatures, the remaining mass was the TiO<sub>2</sub> loading. This way we checked that the nominal TiO<sub>2</sub> % *w/w* loadings were indeed 20% and 40% *w/w*  $\pm 0.5$ –1.0%.

Figure 1 depicts a typical optical microscopy photograph of a 3D printed sample (40% *w/w* TiO<sub>2</sub>/PS), as fabricated following the FDM process mentioned above.



**Figure 1.** Typical photograph of a 3D-printed nanocomposite photocatalytic sample with 40% *w/w* TiO<sub>2</sub> in polystyrene (PS).

As one can notice from Figure 1, rough structures were printed instead of smooth ones, while printing directions were also observed. In our case, the nanoparticle loading (40% *w/w*, shown in Figure 1) in the custom-made filaments, most likely led to low-resolution/low-quality 3D printing. It hence became clear that further investigation was needed in order to improve the printing quality.

Figure 2 presents typical XRD patterns for PS/TiO<sub>2</sub> 3D printed structures. Well-distinguished diffraction peaks are observed. These correspond to both anatase and rutile phase, in good agreement with the JCPDS card (No. 84–1286) and JCPDS card (No. 88–1175), a crystal structure of anatase and rutile, respectively [49,50] normal for P25 Degussa TiO<sub>2</sub> that is a mix of the two phases.

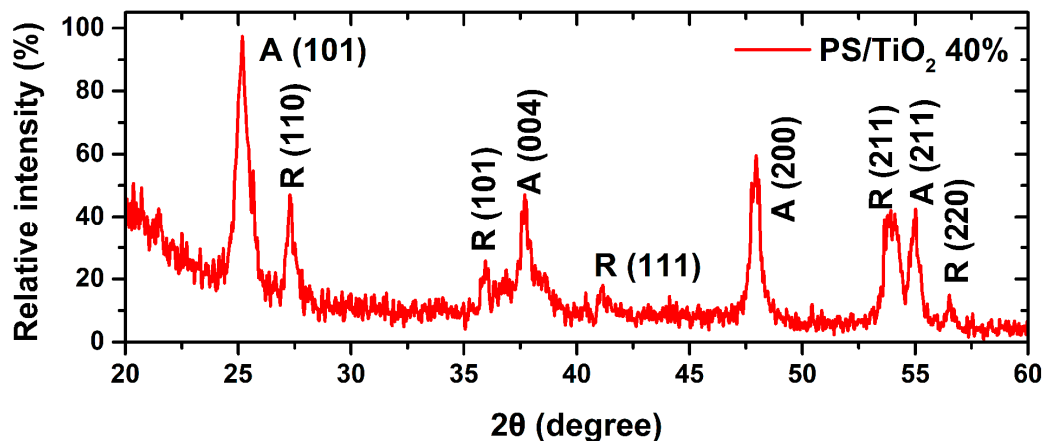


Figure 2. Typical X-ray diffraction (XRD) patterns for PS/TiO<sub>2</sub> 3D-printed nanocomposite structures.

Figure 3 shows a typical Raman spectrum of the PS/TiO<sub>2</sub> 3D printed structures, which exhibit characteristic TiO<sub>2</sub> phonon frequencies, such as: 143 cm<sup>-1</sup> (E<sub>g</sub>), 396 cm<sup>-1</sup> (B<sub>1g</sub>), 516 cm<sup>-1</sup> (A<sub>1g</sub>) for anatase, and 245 cm<sup>-1</sup> (two-phonon scattering) and 610 cm<sup>-1</sup> (A<sub>1g</sub>) for rutile, matching ( $\pm 3$  cm<sup>-1</sup>) with literature [51–53].

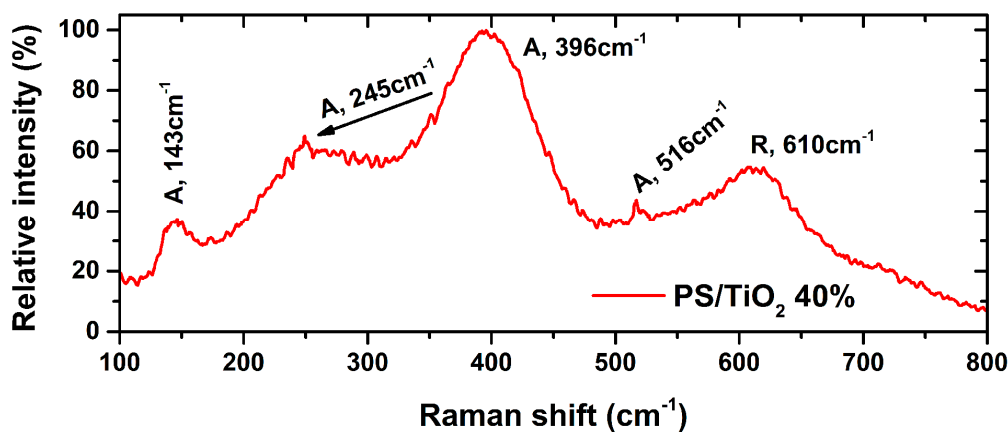
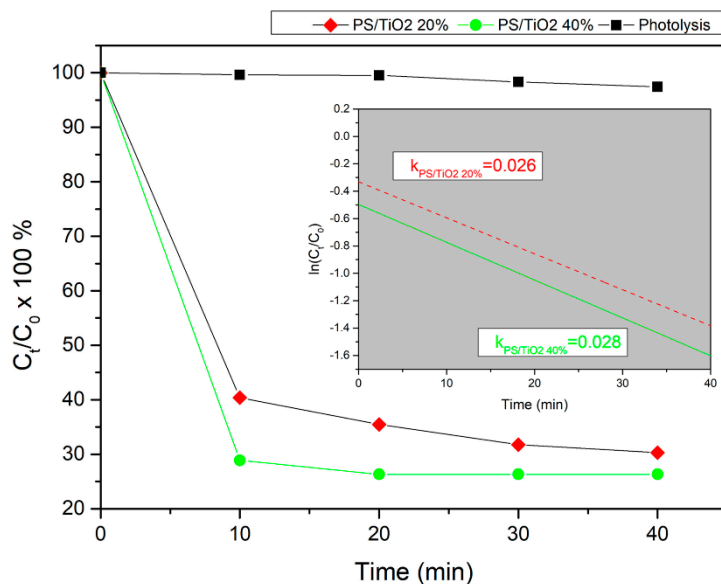


Figure 3. Typical Raman spectra for PS/TiO<sub>2</sub> 3D-printed nanocomposite structures.

The photocatalytic activity of the 3D-printed nanocomposites under UV-A light was evaluated by assessing the reduction of APAP in aqueous solution. The photolytic removal (photolysis) of the pharmaceutical product (in the absence of any photocatalyst) was negligible, underlining the indispensability of the catalysts. Furthermore, to eliminate the possibility of APAP removal by adsorption on the catalysts, the samples were placed at the bottom of the reactor under dark conditions and in contact with the APAP for 30 min, during which time equilibrium of adsorption-desorption was reached. In all cases, removal was insignificant (less than 3%), pointing to the fact that the reduction of the APAP should be attributed to a pure photocatalytic procedure.

The decrease of the concentration of APAP (20 ppm) using both 20% *w/w* and 40% *w/w* 3D-printed TiO<sub>2</sub>/PS nanocomposite samples under UV-A light irradiation is presented in Figure 4. For comparison reasons, the photolysis curve (no catalyst present) is also displayed. According to the photolysis (black curve in Figure 4), the concentration of APAP remained almost constant during ~40 min irradiation, indicating that the photolysis of APAP was almost negligible.



**Figure 4.** Percentage (%) acetaminophen (APAP) degradation using 20% *w/w* and 40% *w/w* [red solid rhombuses and green solid circles] TiO<sub>2</sub>-based 3D-printed nanocomposites under ultraviolet (UV-A) irradiation, vs. irradiation time, respectively. For comparison reasons, the photolysis curve (black solid squares) is also presented. In the inset one can see the apparent rate constants (*k*) of APAP degradation using 20% *w/w* and 40% *w/w* 3D printed TiO<sub>2</sub>/PS nanocomposite photocatalysts.

As shown in Figure 4, the 40% *w/w* 3D-printed TiO<sub>2</sub>/PS nanocomposite photocatalysts were highly effective regarding the reduction of APAP compared to the 20% *w/w* 3D printed TiO<sub>2</sub>/PS nanocomposite ones, due to the highly oxidative radicals generated on the TiO<sub>2</sub> at the surfaces under UV-A irradiation [51].

As already stated, (and shown in the inset of Figure 4), the photodegradation of APAP using the 3D-printed TiO<sub>2</sub>/PS nanocomposite samples followed a first-order kinetics. The calculated apparent rate constants were 0.026 min<sup>-1</sup> and 0.028 min<sup>-1</sup> for 20% *w/w* and 40% *w/w* 3D-printed TiO<sub>2</sub>/PS nanocomposite samples, respectively. One can notice that the 40% *w/w* 3D-printed TiO<sub>2</sub>/PS nanocomposite samples are more photocatalytically active than the 20% *w/w* ones, regarding the degradation of APAP, reaching an almost 30% reduction of APAP's concentration after 10 min of irradiation.

In principle, when a semiconductor is exposed to electromagnetic radiation of an appropriate wavelength, excitation occurs and electrons (e<sub>CB-</sub>) are transferred from the valence band to the conduction band of the material, leaving behind positively charged holes (h<sub>VB+</sub>). The photogenerated holes react with OH<sup>-</sup> or H<sub>2</sub>O adsorbed on the surface of the catalyst, and hydroxyl radicals that are mainly responsible for the degradation of the target pollutant are created. It is therefore expected that a high recombination rate of photogenerated holes and electrons will be disadvantageous for the performance of the photocatalyst.

Nevertheless, an efficient electron and hole transfer between TiO<sub>2</sub> depends on the difference between the conduction and valence band potentials of the semiconductor, that should be suitably positioned [54,55]. Concentration of catalysts in the 40% *w/w* 3D-printed TiO<sub>2</sub>/PS nanocomposite is



double that in the 20% *w/w* 3D-printed TiO<sub>2</sub>/PS nanocomposite samples thus allowing charge separation and increasing the efficiency of the photocatalytic reaction.

In addition, the apparent rate constant (*k*) has been calculated as the basic kinetic parameter for the comparison of photocatalytic activities, which was fitted by the equation  $\ln(C_t/C_0) = -kt$ , where *k* is apparent rate constant, *C<sub>t</sub>* is the concentration of APAP, and *C<sub>0</sub>* is the initial concentration of APAP. It should be noted that the adjusted R-square statistic varies from 0.91499 to 0.94334 indicating that the model used for the determination of the apparent rate constant (*k*) is adequate. The good linear fit of equation  $\ln(C_t/C_0) = -kt$  shown in the inset of Figure 4, confirms that the photodegradation for all different concentrations of APAP using 3D printed TiO<sub>2</sub>/PS nanocomposite photocatalysts at 20% and 40% *w/w*, follows first-order kinetics.

It is worth mentioning that the photocatalytic activity tests were carried out at least three times on the 3D-printed TiO<sub>2</sub>/PS nanocomposite samples to examine their stability under UV illumination, demonstrating no changes in the photocatalytic activity after three runs. Moreover, at least three structures with the same TiO<sub>2</sub> load have been produced and tested, in order to check the reproducibility of the structure manufacturing.

Furthermore, the photocatalytic activity of 40% *w/w* 3D-printed TiO<sub>2</sub>/PS nanocomposite was checked in APAP aqueous solutions with different concentrations (from 20 ppm to 200 ppm). As can be observed from Figure 5a, when the concentration of APAP increases, more irradiation time is needed for its degradation. Although this is expected, it is worth mentioning that for a 100 ppm APAP solution, 20 min of irradiation are enough to reduce it at ~75%, while for 200 ppm APAP solution, 40 min are enough in order to reduce it by the same amount.

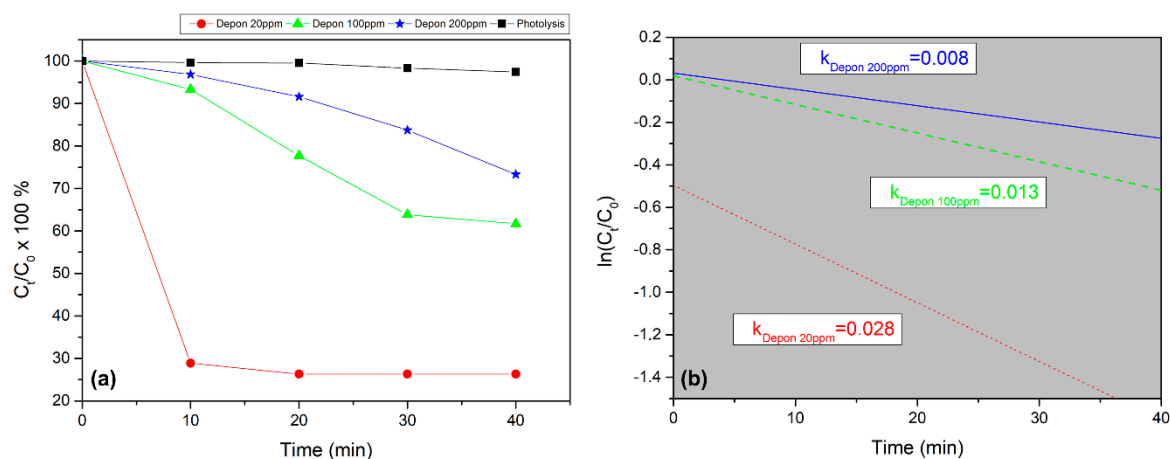


**Figure 5.** (a) % APAP degradation using 40% *w/w* 3D-printed TiO<sub>2</sub>/PS nanocomposites under UV-A irradiation, vs. irradiation time. Three different concentrations of APAP are presented; 20 ppm, 100 ppm and 200 ppm (red solid circles, green solid triangles and blue solid stars, respectively). (b) The apparent rate constants (*k*) of APAP degradation (20 ppm, 100 ppm, and 200 ppm, respectively), using 40% *w/w* 3D printed TiO<sub>2</sub>/PS nanocomposite photocatalysts.

Figure 5b confirms that the photodegradation of APAP using 3D printed TiO<sub>2</sub>/PS nanocomposite samples follow the first-order kinetics. The constant *k* as was calculated (as described above) to be 0.008 min<sup>-1</sup>, 0.013 min<sup>-1</sup> and 0.028 min<sup>-1</sup> for 200 ppm, 100 ppm and 20 ppm of APAP, respectively.

To verify the use of the 3D-printed TiO<sub>2</sub>/PS nanocomposite photocatalysts for practical environmental applications, each sample was recovered, and their efficiency tested for at least three runs. Figure 6 depicts the re-use of one of the 40% *w/w* 3D-printed TiO<sub>2</sub>/PS nanocomposite for three runs, against the degradation of 100 ppm APAP aqueous solution.

As one can see from Figure 6, the 3D-printed TiO<sub>2</sub>/PS nanocomposite photocatalysts can be successfully used at least 3 times for the photodegradation of APAP, reaching an efficiency of ~60% at the end of the 3rd run.

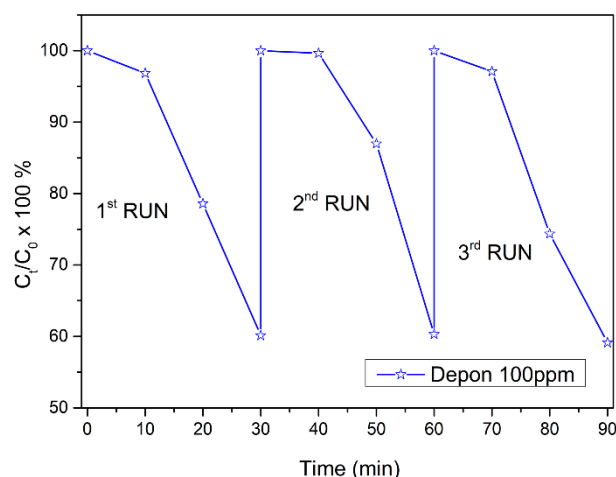


**Figure 6.** % APAP (100 ppm) degradation using a 40% *w/w* TiO<sub>2</sub>/PS 3D-printed nanocomposite sample under UV-A irradiation, for 3 runs of 30 min irradiation each.

#### 4. Summary and Conclusions

This work provides a novel experimental study concerning the successful use of TiO<sub>2</sub>/PS nanocomposite polymeric filaments based on 100% recycled solid polystyrene everyday products, enriched with TiO<sub>2</sub> nanoparticles with mass concentrations up to 40%*w/w*, for the production of 3D photocatalytic structures/devices using a typical FDM-type 3D printer. The 3D-printed TiO<sub>2</sub>/PS nanocomposites were successfully used as photocatalysts for the APAP degradation. It should be noted that this is the first report of 3D-printed photocatalytic devices made of fully recycled raw materials, and with a TiO<sub>2</sub> loading as high as 40% *w/w*.

The 3D-printed TiO<sub>2</sub>/PS nanocomposite samples provide promising photocatalytic properties, reaching an efficiency of almost 60% after three cycles of reuse in 200 ppm of APAP aqueous solution under UV-A irradiation, offering a novel low-cost alternate way for fabricating large-scale photocatalysts, suitable for practical applications.

**Author Contributions:** G.K. developed the original concept. M.S. and G.K. performed the material synthesis and fabrication experiments. M.S., M.P.S. and G.K. carried out the structure characterization, and the photocatalysis experiments and data analysis and processing. G.K. supervised and coordinated the experimental work. All authors have read and agreed to the published version of the manuscript.

**Funding:** This work was supported by the National Priorities Research Program grant No. NPRP11S-1128-170042 from the Qatar National Research Fund (member of The Qatar Foundation), and co-financed by the European Union and Greek national funds through the Operational Program Competitiveness, Entrepreneurship and Innovation, under the call RESEARCH-CREATE-INNOVATE (acronym: POLYSHIELD; project code: T1EDK-02784).

**Acknowledgments:** M.P.S. contribution to this work was partially supported by the Ministry of Education and Research through Program 1—Development of the National R&D System, Subprogram 1.2—Institutional Performance—Projects for Excellence Financing in RDI, EXCEL-IMT, Contract no. 13 PFE/16.10.2018.

**Conflicts of Interest:** The authors declare that there are no conflicts of interest regarding the publication of this manuscript.

#### References

1. Kwon, C.H.; Shin, H.; Kim, J.H.; Choi, W.S.; Yoon, K.H. Degradation of methylene blue via photocatalysis of titanium dioxide. *Mater. Chem. Phys.* **2004**, *86*, 78–82. [[CrossRef](#)]
2. Arabatzis, M.; Antonaraki, S.; Stergiopoulos, T.; Hiskia, A.; Papaconstantinou, E.; Bernard, M.C.; Falaras, P. Preparation, characterization and photocatalytic activity of nanocrystalline thin film TiO<sub>2</sub> catalysts towards 3,5-dichlorophenol degradation. *J. Photochem. Photobiol. A Chem.* **2002**, *149*, 237–245. [[CrossRef](#)]
3. Alberici, R.M.; Jardim, W.F. Photocatalytic destruction of VOCs in the gas-phase using titanium dioxide. *Appl. Catal. B Environ.* **1997**, *14*, 55–68. [[CrossRef](#)]



4. Desale, A.; Kamble, S.P.; Deosarkar, M.P. Photocatalytic Degradation of Paracetamol Using Degussa TiO<sub>2</sub> Photocatalyst. *IJCPS* **2013**, *2*, 140–148.
5. Suryawanshia, M.A.; Maneb, V.B.; Kumbharc, G.B. Immersed Water Purifier: A Novel Approach towards Purification. *Int. J. Innov. Emerg. Res. Eng.* **2016**, *3*, 1–5.
6. Yang, L.; Yu, L.E.; Ray, M.B. Degradation of paracetamol in aqueous solutions by TiO<sub>2</sub> photocatalysis. *Water Res.* **2008**, *42*, 3480–3488. [[CrossRef](#)]
7. Shakir, M.; Faraz, M.; Sherwani, M.A.; Al-Resayes, S.I. Photocatalytic degradation of the Paracetamol drug using Lanthanum doped ZnO nanoparticles and their in-vitro cytotoxicity assay. *J. Lumin.* **2016**, *176*, 159–167. [[CrossRef](#)]
8. Thi, V.H.T.; Lee, B.K. Effective photocatalytic degradation of paracetamol using La-doped ZnO photocatalyst under visible light irradiation. *Mater. Res. Bull.* **2017**, *96*, 171–182. [[CrossRef](#)]
9. Cifci, D.I.; Tuncal, T.; Pala, A.; Uslu, O. Determination of optimum extinction wavelength for paracetamol removal through energy efficient thin film reactor. *J. Photochem. Photobiol. A Chem.* **2016**, *322–323*, 102–109.
10. Patil, S.S.; Shinde, V.M. Biodegradation studies of aniline and nitrobenzene in aniline plant wastewater by gas chromatography. *Environ. Sci. Technol.* **1988**, *22*, 1160–1165. [[CrossRef](#)]
11. More, A.T.; Vira, A.; Fogel, S. Biodegradation of trans-1,2-dichloroethylene by methane-utilizing bacteria in an aquifer simulator. *Environ. Sci. Technol.* **1989**, *23*, 403–406.
12. Slokar, Y.M.; Le Marechal, A.M. Methods of decoloration of textile wastewaters. *Dye. Pigment.* **1998**, *37*, 335–356.
13. Bahadur, N.; Jain, K.; Srivastava, A.K.; Govind, R.; Gakhar, D.; Haranath; Dulat, M.S. Effect of nominal doping of Ag and Ni on the crystalline structure and photo-catalytic properties of mesoporous titania. *Mater. Chem. Phys.* **2010**, *124*, 600–608.
14. Soutsas, K.; Karayannis, V.; Poullos, I.; Riga, A.; Ntampegliotis, K.; Spiliotis, X.; Papapolymerou, G. Decolorization and degradation of reactive azo dyes via heterogeneous photocatalytic processes. *Desalination* **2010**, *250*, 345–350.
15. Peng, Y.H.; Huang, G.F.; Huang, W.Q. Visible-light absorption and photocatalytic activity of Cr-doped TiO<sub>2</sub> nanocrystal films. *Adv. Powder Technol.* **2012**, *23*, 8–12.
16. Hashimoto, K.; Irie, H.; Fujishima, A. TiO<sub>2</sub> Photocatalysis: A Historical Overview and Future Prospects. *Jpn. J. Appl. Phys.* **2005**, *44*, 8269–8285.
17. Carp, O.; Huisman, C.L.; Reller, A. Photoinduced reactivity of titanium dioxide. *Prog. Solid State Chem.* **2004**, *32*, 33–177.
18. Kenanakis, G.; Giannakoudakis, Z.; Vernardou, D.; Savvakis, C.; Katsarakis, N. Photocatalytic degradation of stearic acid by ZnO thin films and nanostructures deposited by different chemical routes. *Catal. Today* **2010**, *151*, 34–38.
19. Chen, X.; Wu, Z.; Liu, D.; Gao, Z. Preparation of ZnO Photocatalyst for the Efficient and Rapid Photocatalytic Degradation of Azo Dyes. *Nanoscale Res. Lett.* **2017**, *12*, 1–10.
20. Frysalis, M.A.; Papoutsakis, L.; Kenanakis, G.; Anastasiadis, S.H. Functional Surfaces with Photocatalytic Behavior and Reversible Wettability: ZnO Coating on Silicon Spikes. *J. Phys. Chem. C* **2015**, *119*, 25401–25407.
21. Yu, K.S.; Shi, J.Y.; Zhang, Z.L.; Liang, Y.M.; Liu, W. Synthesis, Characterization, and Photocatalysis of ZnO and Er-Doped ZnO. *J. Nanomater.* **2013**. [[CrossRef](#)]
22. Johar, M.A.; Afzal, R.A.; Alazba, A.A.; Manzoor, U. Photocatalysis and bandgap engineering using ZnO nanocomposites. *Adv. Mater. Sci. Eng.* **2015**. [[CrossRef](#)]
23. Kenanakis, G.; Katsarakis, N. Light-induced photocatalytic degradation of stearic acid by c-axis-oriented ZnO nanowires. *Appl. Catal. A* **2010**, *378*, 227–233. [[CrossRef](#)]
24. Kenanakis, G.; Vernardou, D.; Katsarakis, N. Light-induced self-cleaning properties of ZnO nanowires grown at low temperatures. *Appl. Catal. A* **2012**, *411*, 7–14. [[CrossRef](#)]
25. Aguilar, C.A.; Montalvo, C.; Ceron, J.G.; Moctezuma, E. Photocatalytic Degradation of Acetaminophen. *Int. J. Environ. Res.* **2011**, *5*, 1071–1078.
26. Konstantinou, I.; Albanis, T. Photocatalytic Transformation of Pesticides in Aqueous Titanium Dioxide Suspensions Using Artificial and Solar Light: Intermediates and Degradation Pathways. *Appl. Catal. B* **2003**, *42*, 319–335. [[CrossRef](#)]
27. Tanaka, K.; Padermpole, K.; Hisanaga, T. Photocatalytic Degradation of Commercial Azo Dyes. *Water Res.* **2000**, *34*, 327–333. [[CrossRef](#)]

28. Mills, A.; Lee, S. A web-based overview of semiconductor photochemistry-based current commercial applications. *J. Photochem. Photobiol A Chem.* **2002**, *152*, 233–247. [[CrossRef](#)]
29. Li, Y.; Chen, J.; Liu, J.; Ma, M.; Chen, W.; Li, L. Activated carbon supported TiO<sub>2</sub>-photocatalysis doped with Fe ions for continuous treatment of dye wastewater in a dynamic reactor. *J. Environ. Sci.* **2010**, *22*, 1290–1296. [[CrossRef](#)]
30. Van Grieken, R.; Marugán, J.; Sordo, C.; Martínez, P.; Pablos, C. Photocatalytic inactivation of bacteria in water using suspended and immobilized silver-TiO<sub>2</sub>. *Appl. Catal. B Environ.* **2009**, *93*, 112–118. [[CrossRef](#)]
31. Banerjee, A.N.; Ghosh, C.K.; Chattopadhyay, K.K.; Minoura, H.; Sarkar, A.K.; Akiba, A.; Kamiya, A.; Endo, T. Low-temperature deposition of ZnO thin films on PET and glass substrates by DC-sputtering technique. *Thin Solid Films* **2006**, *496*, 112–116. [[CrossRef](#)]
32. Zhao, J.; Chen, C.; Ma, W. Photocatalytic Degradation of Organic Pollutants Under Visible Light Irradiation. *Top. Catal.* **2005**, *35*, 269–278. [[CrossRef](#)]
33. Mills, A.; Elliott, N.; Hill, G.; Fallis, D.; Durrant, J.R.; Willis, R.L. Preparation and characterisation of novel thick sol-gel titania film photocatalysts. *Photochem. Photobiol. Sci.* **2003**, *2*, 591–596. [[CrossRef](#)]
34. Henderson, M.A. A surface science perspective on TiO photocatalysis. *Surf. Sci. Rep.* **2011**, *66*, 185–297. [[CrossRef](#)]
35. Lopez, L.; Daoud, W.A.; Dutta, D. Preparation of large scale photocatalytic TiO<sub>2</sub> films by the sol-gel process. *Surf. Coat. Technol.* **2010**, *2*, 251–257. [[CrossRef](#)]
36. Beltrame, E.D.V.; Tyrwhitt-Drake, J.; Roy, I.; Shalaby, R.; Suckale, J.; Pomeranz Krummel, D. 3D Printing of Biomolecular Models for Research and Pedagogy. *J. Vis. Exp.* **2017**, *121*, 55427.
37. Ventola, C.L. Medical Applications for 3D Printing: Current and Projected Uses. *Pharm. Ther.* **2014**, *39*, 704–711.
38. Lee, J.Y.; An, J.; Chua, C.K. Fundamentals and applications of 3D printing for novel materials. *Appl. Mater. Today* **2017**, *7*, 120–133. [[CrossRef](#)]
39. Ambrosi, A.; Pumera, M. 3D-printing technologies for electrochemical applications. *Chem. Soc. Rev.* **2016**, *45*, 2740–2755. [[CrossRef](#)]
40. Kenanakis, G.; Vasilopoulos, K.C.; Viskadourakis, Z.; Barkoula, N.M.; Anastasiadis, S.H.; Kafesaki, M.; Economou, E.N.; Soukoulis, C.M. Electromagnetic shielding effectiveness and mechanical properties of graphite-based polymeric films. *Appl. Phys. A* **2016**, *122*, 802–810. [[CrossRef](#)]
41. Lee, H.U.; Lee, S.C.; Lee, Y.C.; Son, B.; Park, S.Y.; Lee, J.W.; Oh, Y.K.; Kim, Y.; Choi, S.; Lee, Y.S.; et al. Innovative three-dimensional (3D) eco-TiO<sub>2</sub> photocatalysts for practical environmental and bio-medical applications. *Sci. Rep.* **2014**, *4*, 6740. [[CrossRef](#)] [[PubMed](#)]
42. Hernández-Afonso, L.; Fernández-González, R.; Esparza, P.; Borges, M.E.; Dí González, S.; Canales-Vázquez, J.; Ruiz-Morales, J.C. Three dimensional printing of components and functional devices for energy and environmental applications. *Energy Environ. Sci.* **2017**, *10*, 846–859.
43. Giakoumaki, A.N.; Kenanakis, G.; Klini, A.; Androulidaki, M.; Viskadourakis, Z.; Farsari, M.; Selimis, A. 3D micro-structured arrays of ZnO nanorods. *Sci. Rep.* **2017**, *7*, 2100. [[CrossRef](#)]
44. Skorski, M.R.; Esenther, J.M.; Ahmed, Z.; Miller, A.E.; Hartings, M.R. The chemical, mechanical, and physical properties of 3D printed materials composed of TiO<sub>2</sub>-ABS nanocomposites. *Sci. Technol. Adv. Mater.* **2016**, *17*, 89–97. [[CrossRef](#)] [[PubMed](#)]
45. Viskadourakis, Z.; Sevastaki, M.; Kenanakis, G. 3D structured nanocomposites by FDM process: A novel approach for large-scale photocatalytic applications. *Appl. Phys. A* **2018**, *124*, 585–593. [[CrossRef](#)]
46. Al-Kaf, A.G.; Naji, K.M.; Abdullah, Q.Y.M.; Edrees, W.H.A. Occurrence of Paracetamol in Aquatic Environments and Transformation by Microorganisms: A Review. *Chron. Pharm. Sci.* **2017**, *1*, 341–355.
47. Jones, O.A.H.; Voulvoulis, N.; Lester, J.N. The occurrence and removal of selected pharmaceutical compounds in a sewage treatment works utilizing activated sludge treatment. *Environ. Pollut.* **2007**, *145*, 738–744. [[CrossRef](#)]
48. Żur, J.; Piński, A.; Marchlewicz, A.; Hupert-Kocurek, K.; Wojcieszynska, D.; Guzik, U. Organic micropollutants paracetamol and ibuprofen—toxicity, biodegradation, and genetic background of their utilization by bacteria. *Environ. Sci. Pollut. Res.* **2018**, *25*, 21498–21524. [[CrossRef](#)]
49. Sadeghzadeh-Attar, A.; Ghamsari, M.S.; Hajiesmaeilbaigi, F.; Mirdamadi, S.; Katagiri, K.; Koumoto, K. Modifier ligands effects on the synthesized TiO<sub>2</sub> nanocrystals. *J. Mater. Sci.* **2008**, *43*, 1723–1729. [[CrossRef](#)]

50. Bakardjieva, S.; Šubrt, J.; Štengl, V.; Dianez, M.J.; Sayagues, M.J. Photoactivity of Anatase-Rutile TiO<sub>2</sub> Nanocrystalline Mixtures Obtained by Heat Treatment of Homogeneously Precipitated Anatase. *Appl. Catal. B Environ.* **2005**, *58*, 193–202. [[CrossRef](#)]
51. Lubas, M.; Jasinski, J.J.; Sitarz, M.; Kurpaska, L.; Podsiad, P.; Jasinski, J. Raman spectroscopy of TiO<sub>2</sub> thin films formed by hybrid treatment for biomedical applications. *Spectrochim. Acta Part A* **2014**, *133*, 867–871. [[CrossRef](#)] [[PubMed](#)]
52. Shaikh, S.F.; Mane, R.S.; Min, B.K.; Hwang, Y.J.; Joo, O. D-sorbitol-induced phase control of TiO<sub>2</sub> nanoparticles and its application for dye-sensitized solar cells. *Sci. Rep.* **2016**, *6*, 20103. [[CrossRef](#)]
53. Shinde, D.V.; Patil, S.A.; Cho, K.; Ahn, D.Y.; Shrestha, N.K.; Mane, R.S.; Lee, J.K.; Han, S.H. Revisiting Metal Sulfide Semiconductors: A Solution-Based General Protocol for Thin Film Formation, Hall Effect Measurement, and Application Prospects. *Adv. Funct. Mater.* **2015**, *25*, 5739–5747. [[CrossRef](#)]
54. Sunada, K.; Kikuchi, Y.; Hashimoto, K.; Fujishima, A. Bactericidal and Detoxification Effects of TiO<sub>2</sub> Thin Film Photocatalysts. *Environ. Sci. Technol.* **1998**, *32*, 726–728. [[CrossRef](#)]
55. Rehman, S.; Ullah, R.; Butt, A.M.; Gohar, N.D. Strategies of making TiO<sub>2</sub> and ZnO visible light active. *J. Hazard. Mater.* **2009**, *170*, 560–569. [[CrossRef](#)]

**Publisher's Note:** MDPI stays neutral with regard to jurisdictional claims in published maps and institutional affiliations.



© 2020 by the authors. Licensee MDPI, Basel, Switzerland. This article is an open access article distributed under the terms and conditions of the Creative Commons Attribution (CC BY) license (<http://creativecommons.org/licenses/by/4.0/>).